

Supplemental Materials

Molecular Biology of the Cell

Zhao et al.

Supplemental Figure S1. Strategy for screening recessive mutations on 2L.

(A) The second chromosome of *ey-flp,Rh1-GFP;FTR40A* flies was isogenized and flies were mutagenized by feeding 25 mM EMS (Sigma) in 2% sucrose for 8 h. They were then mated to *ey-flp Rh1-GFP;GMR-hid CL FRT40A/Cyo hs-hid* flies. Flies were heat shocked at 37°C for 1 h to avoid having heterozygous flies among the F1 progeny (the pro-apoptosis gene *hid* was induced by heat-shock (*hs-hid*) in heterozygous flies). The DPP was assessed in F1 flies using a fluorescent stereo microscope day 1 and 5 following eclosion.

Supplemental Figure S2. Alignment of different *Drosophila* Vha68 proteins.

Amino acid sequences of *Drosophila* Vha68-1, Vha68-2, and Vha68-3, as well as human ATP6V1A are shown. Identical residues, found in at least two proteins, are enclosed in black boxes. The running tally of amino acids is indicated to the right.

Supplemental Figure S3. Decreased light sensitivity and reduced Rh1 levels in *vha68-1¹* flies.

(A) Light sensitivity assay was performed using ~1-day-old wild-type, *vha68-1¹*, and *vha100-1²* flies. Flies were dark-adapted for 2 min before being exposed to five pulses of 5-sec of white light with increasing intensity. The maximal light intensity was 300 Lux (10^{-1}).
(B) Total Rh1 levels were decreased in *vha68-1¹* flies. Head extracts were prepared from 1-day-old flies of indicated genotypes and labeled using antibodies against Rh1 and INAD.
(C) Quantification of Rh1 levels in each genotype. Rh1 levels were normalized to INAD levels, which served as a loading control. $n = 7$, data are presented as mean \pm SD, *** $p < 0.001$ (Student's unpaired t-test).

Supplemental Figure S4. Localization of the scaffold protein INAD and the basolateral membrane protein Na⁺K⁺ATPase were not affected in *vha68-1¹* flies.

(A) Tangential resin-embedded retina sections from ~1-day-old wild type and *vha68-1* flies were labeled using antibodies against Rh1 (green) and INAD (red). The localization pattern of INAD was indistinguishable between control and *vha68-1* flies. Scale bars are 2 μm . (B) Adult eyes from wild type and *vha68-1* flies were dissected and stained with antibodies against $\text{Na}^+\text{K}^+\text{ATPase}$ (red). GFP fluorescence of Rh1-GFP was directly observed to indicate rhabdomeres. The localization pattern of $\text{Na}^+\text{K}^+\text{ATPase}$ was not affected in *vha68-1* flies. Scale bars are 2 μm .

Supplemental Figure S5. Schematic view and representative images of the Rh1 pulse-chase assay.

(A) Schematic shows the Rh1 pulse-chase assay. Newly hatched flies were exposed to 37°C for 1 h, and then placed in the dark. Flies were collected at indicated time points (6, 18, 24, and 48 h) after heat-shock. Rh1-GFP localized in the rhabdomere, marked by green; hs-Rh1-RFP was synthesized in the ER and transported to the rhabdomere, marked by red. N, nuclear; C, Cell body; R, rhabdomere. (B-E) Cryostat sections of *hs-Rh1-RFP/+* and *vha68-1¹;hs-Rh1-RFP/+* heads at 6 (B), 18 (C), 24 (D), and 48 h (E) after heat shock were labeled with antibodies against RFP. GFP fluorescence of Rh1-GFP was directly observed to indicate rhabdomeres. Scale bars are 5 μm .

Supplemental Figure S6. Vha68-1 functions in Rh1 post-Golgi trafficking to rhabdomere.

(A) Cryostat sections of *ninaE-gal4;UAS-shi^{ts1} (ey-flp rh1-GFP;ninaE-gal4/+;hs-rh1-RFP/UAS-shi^{ts1})*, *vha68-1¹ (ey-flp rh1-GFP;vha68-1¹ FRT40A/GMR-hid CL FRT40A; hs-rh1-RFP /+)* and *vha68-1¹ninaE-gal4;UAS-shi^{ts1} (ey-flp rh1-GFP; vha68-1¹ FRT40A ninaE-gal4/GMR-hid CL FRT40A;hs-rh1-RFP/UAS-shi^{ts1})* heads 24 h after heat shock were labeled with antibodies against RFP. GFP fluorescence of Rh1-GFP was directly observed to indicate rhabdomeres. Scale bars are 5 μm . (B) Quantification of rhabdomere-localized, newly synthesized Rh1-RFP at 24 h after heat shock. Six different compound eye sections of each sample were quantified. Error bars

indicate SD, ***p < 0.001; ns, not significant (Student's unpaired t-test). (C) Adult eyes from wild type, *vha68-1¹*, *ninaE-gal4;UAS-shi^{ts1}*, and *vha68-1¹ninaE-gal4;UAS-shi^{ts1}* flies were dissected and stained with antibodies against Rh1 (green). Rh1 vesicles still accumulated in *vha68-1¹* flies in the *shi^{ts1}* background. Scale bars are 5 μ m.

Supplemental Figure S7. Vha100-1 colocalizes with multiple endosome markers in the synaptic terminal in the lamina.

(A) The nSyb-mp reporter and Vha100-1 colocalize in the synaptic terminal in the lamina. Cryostat sections of *nSyb-mp/v100-myc* (*ninaE-nSyb-mCherry-pHluorin/ninaE-vha100-myc*) were labeled with antibodies against Myc (green) and RFP (red). Scale bars are 5 μ m. (B) Cryostat sections of *rab5-RFP/v100-myc* (*ninaE-rab5-RFP/ninaE-vha100-myc*), *rab7-RFP/v100-myc* (*ninaE-rab7-RFP/ninaE-vha100-myc*), *rab11-RFP/v100-myc* (*ninaE-rab11-RFP/ninaE-vha100-myc*), and *lamp1-RFP/v100-GFP* (*ninaE-lamp1-RFP/ninaE-vha100-GFP*) heads were labeled with antibodies against Myc (green) or GFP (green) and RFP (red). Scale bars are 5 μ m.

Supplemental Figure S8. V-ATPase is required to maintain pH in Rh1 secretory vesicles during its trafficking to the rhabdomere and the deglycosylation process.

(A) Tangential resin-embedded retina sections of compound eyes from ~1-day-old wild type, *dmppe^{e02905}*, *vha68-1¹*, and *vha68-1¹ dmppe^{e02905}* flies were labeled using antibodies against Rh1. Scale bars are 2 μ m. (B) Tangential resin-embedded retina sections of compound eyes from ~1-day-old wild type, *vha100-1²*, *ninaE-v100-GFP;vha100-1²* (*ey-flp rh1-GFP; ninaE-vha100-1-GFP/+;vha100-1² FRT82B/GMR-hid CL FRT82B*), and *ninaE-v100^{R755A}-GFP;vha100-1²* (*ey-flp rh1-GFP; ninaE-vha100-1^{R755A}-GFP/+;vha100-1² FRT82B/GMR-hid CL FRT82B*) flies were labeled using antibodies against Rh1. Scale bars are 2 μ m. (C) Head extracts were prepared from ~1-day-old wild type, *vha100-1²*, *ninaE-v100-GFP;vha100-1²*, and *ninaE-v100^{R755A}-GFP;vha100-1²* flies and labeled with antibodies against Rh1.

V-ATPase subunit	mutation	phenotype
<i>vha100</i>	<i>vha100-1</i> ¹	No ERG transient
<i>vha100</i>	<i>vha100-1</i> ²	No ERG transient
<i>vhaSFD</i>	<i>vhaSFD</i> ^{EY04644}	No homozygous eye
<i>vha68-2</i>	<i>vha68-2</i> ^{S4214}	No homozygous eye
<i>vha68-2</i>	<i>vha68-2</i> ^{EP2364}	No homozygous eye
<i>vha68-2</i>	<i>vha68-2</i> ^{R6}	No homozygous eye
<i>vha44</i>	<i>vha44</i> ^{KG00915}	No homozygous eye
<i>vhaAC39-1</i>	<i>vhaAC39-1</i> ^{FY38}	No homozygous eye
<i>vhaAC39-1</i>	<i>vhaAC39-1</i> ^{FZ29}	No homozygous eye

Table S1: Phenotypes of mutations in V-ATPase genes.All alleles are homozygous lethal, and eyes of homozygous mutations were generated using the “*Rh1::GFPey-flp/hid*” method.

Figure S1

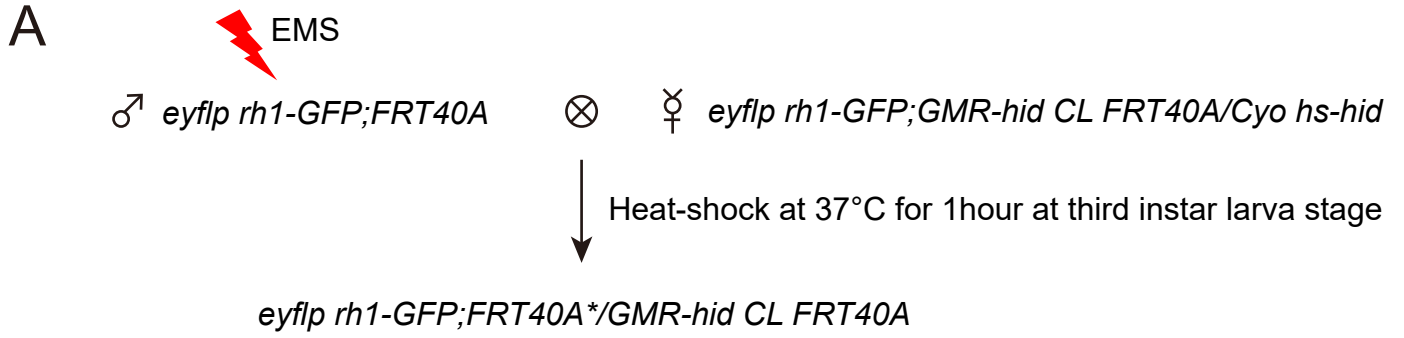


Figure S3

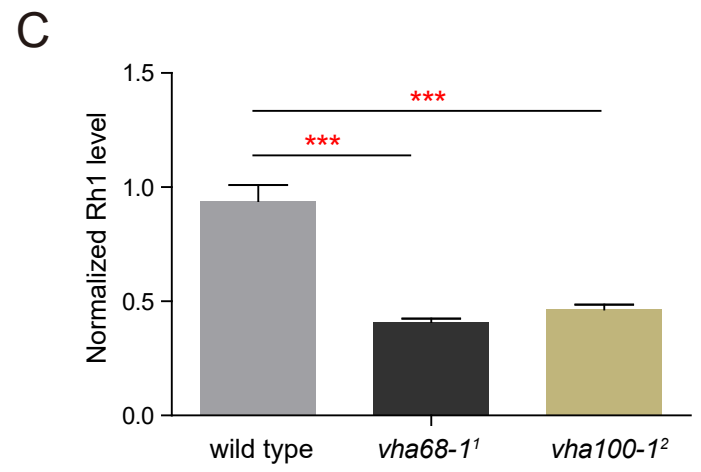
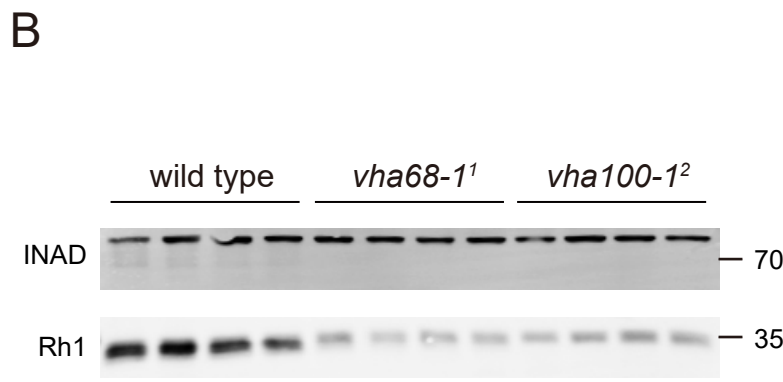
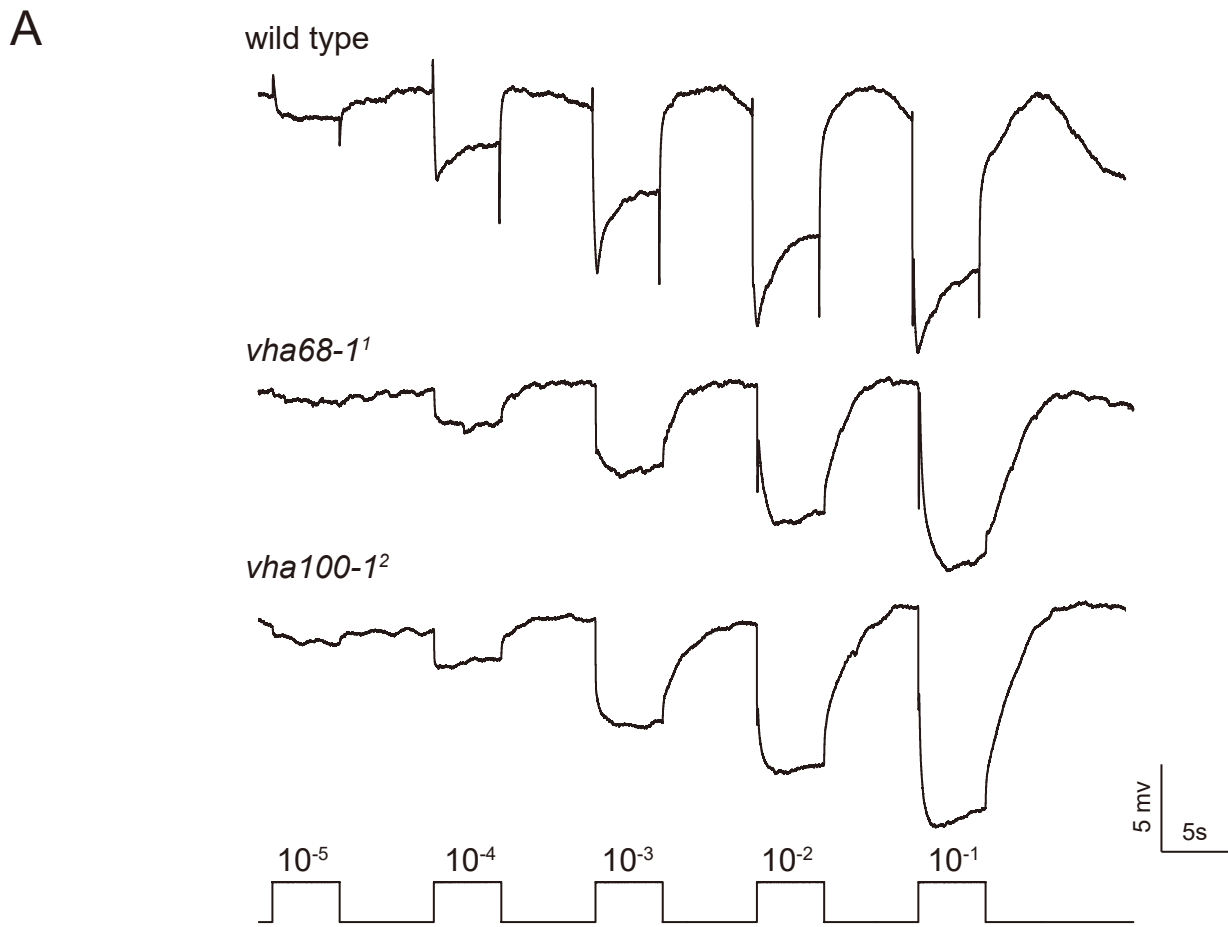
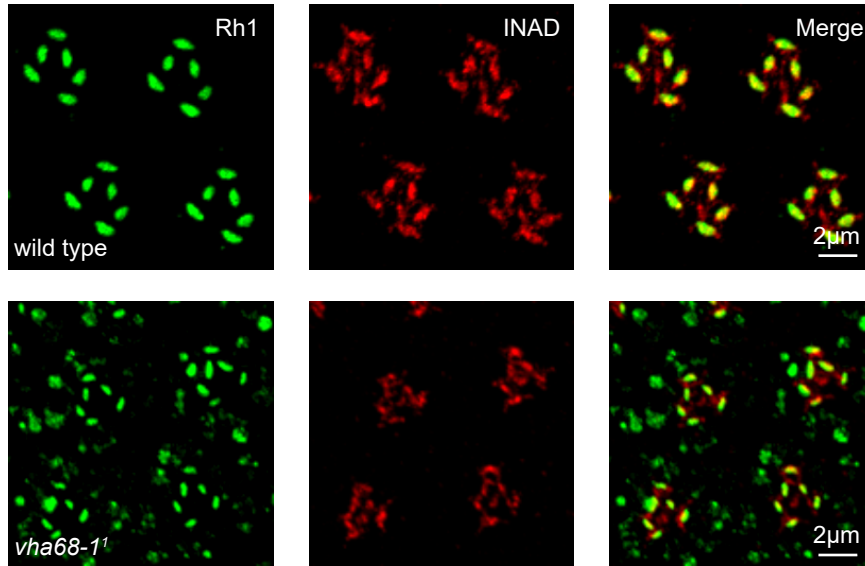


Figure S4

A



B

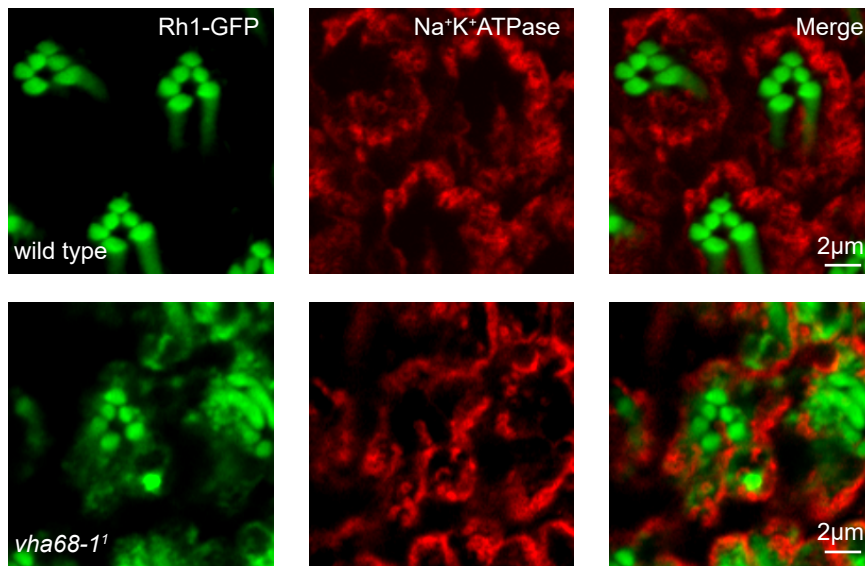
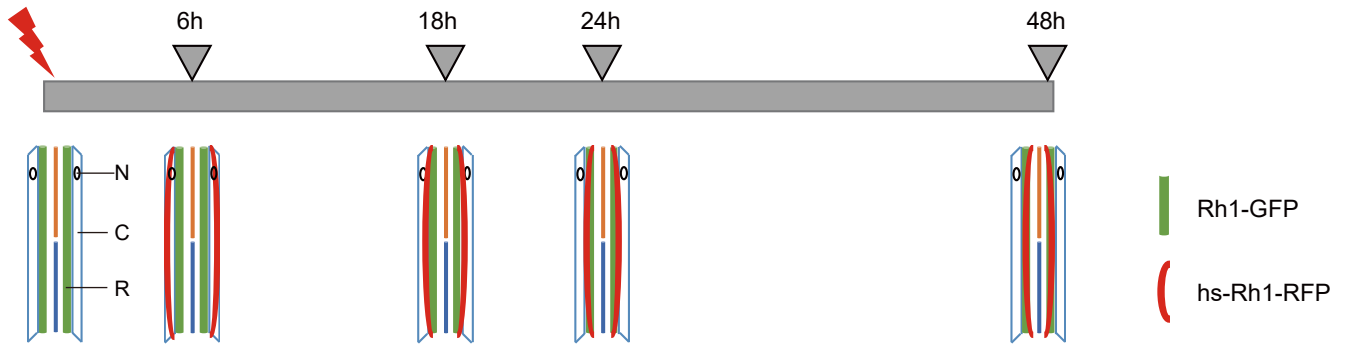


Figure S5

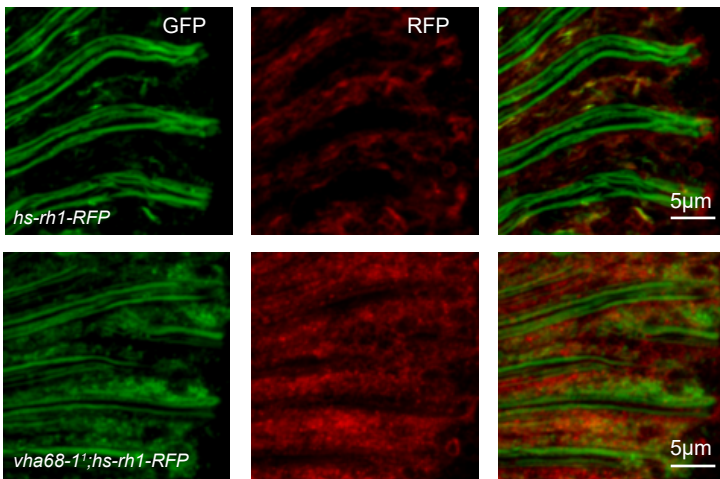
A

37°C heat-shock 1h
raised in dark



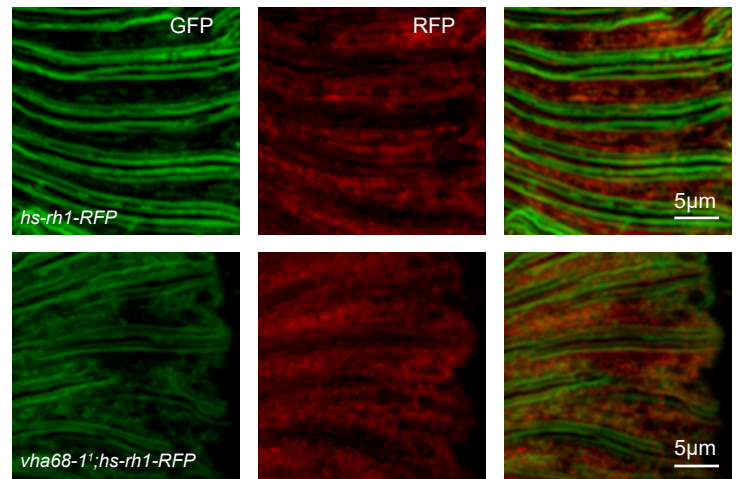
B

6h after heat-shock



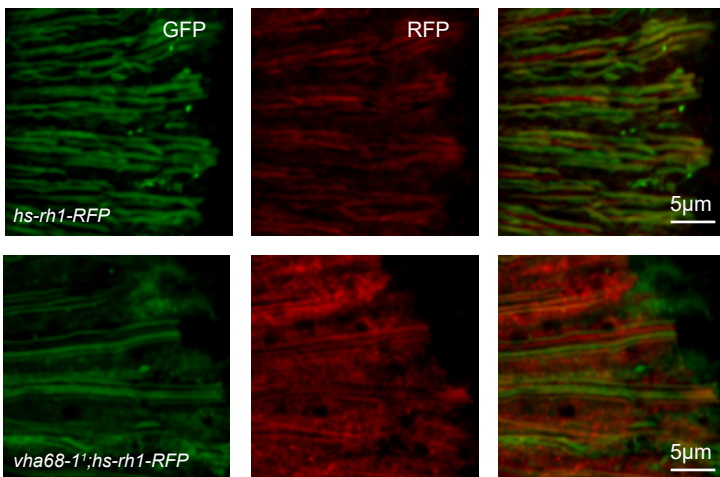
C

18h after heat-shock



D

24h after heat-shock



E

48h after heat-shock

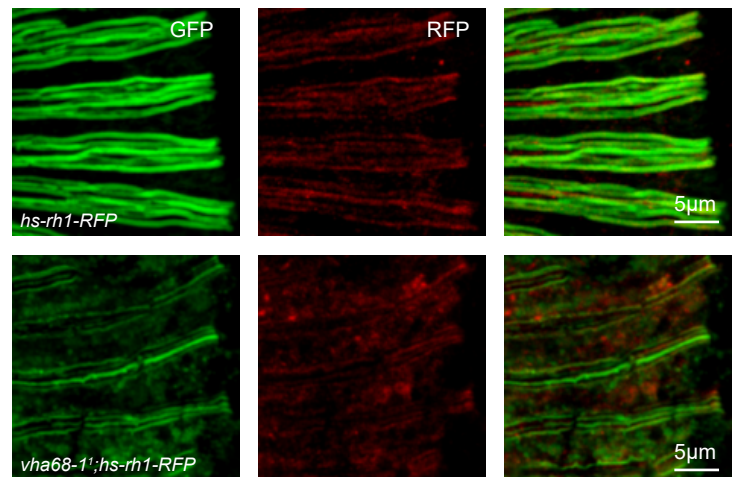
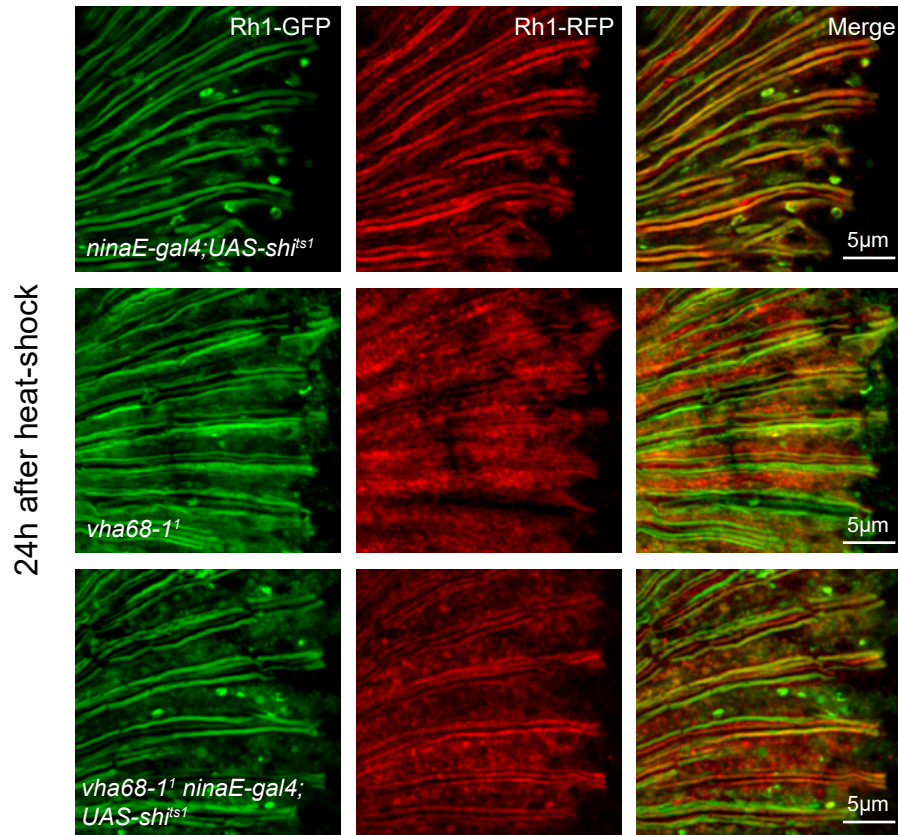
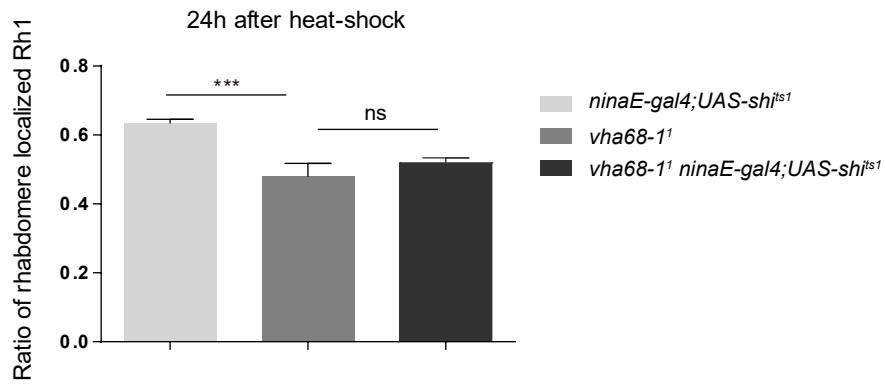


Figure S6

A



B



C

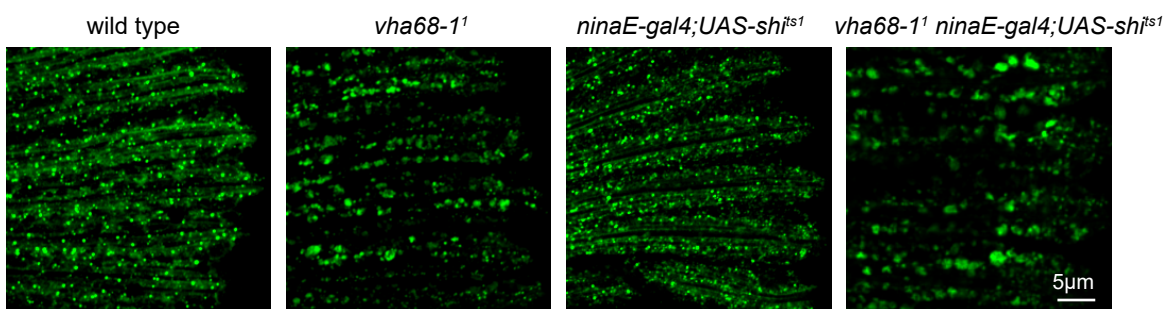
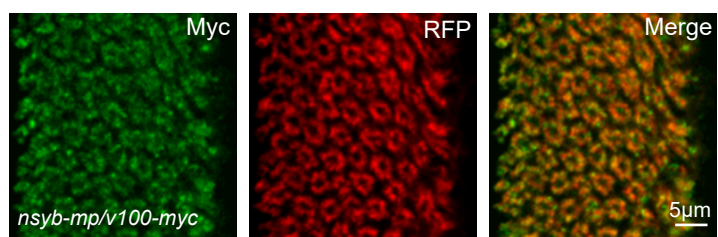


Figure S7

A



B

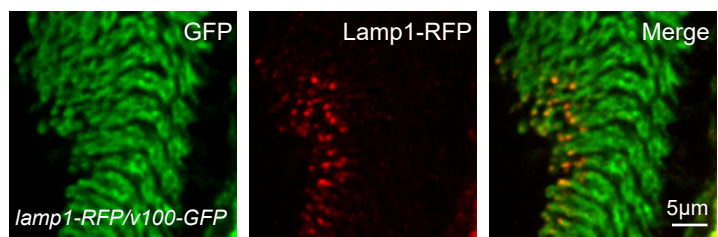
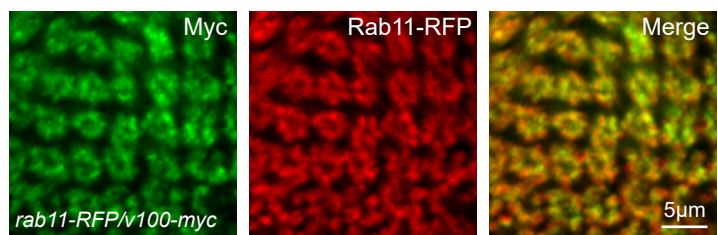
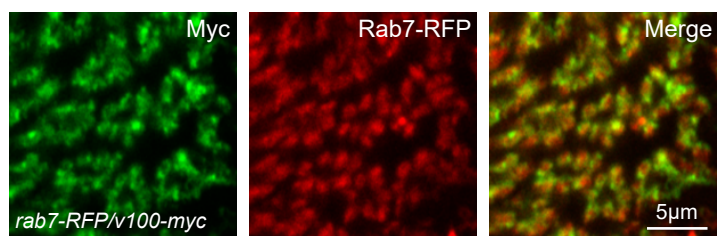
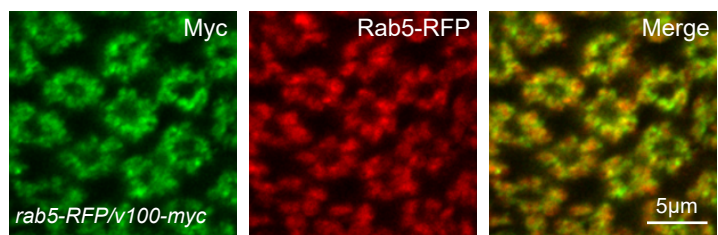


Figure S8

